Atomic Force Microscope Studies of the Fusion of Floating Lipid Bilayers

Midhat H. Abdulreda and Vincent T. Moy
Department of Physiology & Biophysics, University of Miami Miller School of Medicine, Miami, Florida, USA

ABSTRACT This study investigated the fusion of apposing floating bilayers of egg L-α-phosphatidylcholine (egg PC) or 1,2-dimyristoyl-*sn*-glycero-3-phosphocholine. Atomic force microscope measurements of fusion forces under different compression rates were acquired to reveal the energy landscape of the fusion process under varied lipid composition and temperature. Between compression rates of ~1000 and ~100,000 pN/s, applied forces in the range from ~100 to ~500 pN resulted in fusion of floating bilayers. Our atomic force microscope measurements indicated that one main energy barrier dominated the fusion process. The acquired dynamic force spectra were fit with a simple model based on the transition state theory with the assumption that the fusion activation potential is linear. A significant shift in the energy landscape was observed when bilayer fluidity and composition were modified, respectively, by temperature and different cholesterol concentrations (15% $\leq$ chol $\leq$ 25%). Such modifications resulted in a more than twofold increase in the width of the fusion energy barrier for egg PC and 1,2-dimyristoyl-*sn*-glycero-3-phosphocholine floating bilayers. The addition of 25% cholesterol to egg PC bilayers increased the activation energy by ~1.0 k_BT compared with that of bilayers with egg PC alone. These results reveal that widening of the energy barrier and consequently reduction in its slope facilitated membrane fusion.

INTRODUCTION

Membrane fusion is essential for survival in eukaryotic cells and organisms. Transmitter release, cellular trafficking, and compartmentalization, endocytosis and exocytosis, and sexual reproduction are examples of the many physiologic processes that depend directly or indirectly on membrane fusion (1,2). Conversely, certain pathologic conditions may also arise due to excessive release or defects in the fusion process (3,4). Supported lipid membranes have been extensively used as model systems for biological membranes in the investigation of their interactions in an effort to understand mechanisms of membrane fusion (5–10).

The atomic force microscope (AFM) has been used to image and investigate supported lipid bilayers (11–13). Since its introduction by Binnig et al. (1986) as a high resolution imaging device (14–19), the AFM has proven to be a very powerful apparatus capable of measuring surface and intermolecular forces in the piconewton range (20–22). Recently, the AFM was used to investigate interactions between two solid supported lipid bilayers, where a surface modification of the silicon nitride cantilever tip was performed to ensure reliable and reproducible bilayer formation (23).

Emerging studies have characterized floating bilayers and support their application as improved models for lipid membranes (24,25). Floating bilayers float ~2.5 nm on top supported bilayers (26,27). Because the floating bilayers are further away from the underlying support, the coupling between the substrate and the floating bilayers is reduced, making them more comparable to biological membranes (28). Floating bilayers have been formed mainly by Langmuir-Blodgett deposition followed by a Langmuir-Schaeffer deposition on top of the supported bilayers (29). In the last few years, however, several articles appeared in the literature where double bilayers (i.e., floating on top of supported) were formed by vesicle adsorption onto hydrophilic substrates (26,30–33).

This work was designed to study the fusion of apposing floating bilayers. The effects of temperature and lipid composition on the interaction forces between bilayers were investigated. The kinetics of the fusion process for bilayers prepared from 1,2-dimyristoyl-*sn*-glycero-3-phosphocholine (DMPC) or egg L-α-phosphatidylcholine (egg PC; with and without cholesterol) were revealed. Using AFM, fusion force scan measurements were carried out under different compression rates, and plots of force versus compression rate were generated. Our measurements indicated that the fusion force is proportional to the natural logarithm of the compression rate (34). This is consistent with a model where the energy barrier between the interacting bilayers decreases linearly with applied compression force. Under the current conditions, fitting the model to the data revealed that the fusion of apposing floating membranes was governed by one main energy barrier, which strongly depended on the fluidity and lipid composition of the interacting bilayers. The fusion rate constant, in the absence of compression force, and the width of the energy barrier were derived from the model and used to compare the activation energy of the fusion process in the different experimental conditions.

MATERIALS AND METHODS

Materials

Solutions (in chloroform) of egg L-α-phosphatidylcholine (egg PC), 1,2-dimyristoyl-*sn*-glycero-3-phosphocholine (DMPC), and 1,2-dipalmitoyl-sn-glycero-3-phosphoethanolamine-*N*-(7nito-2-1,3-benzoxadiazol-4-yl) (NBD-PE)

Submitted August 31, 2006, and accepted for publication February 13, 2007.

Address reprint requests to Vincent T. Moy, University of Miami Miller School of Medicine, Physiology & Biophysics Department, 1600 NW 10th Ave. Miami, FL 33136. Tel.: 305-243-3201; Fax: 305-243-5931; E-mail: vmoy@miami.edu.

0006-3495/07/06/4369/10 $2.00

doi: 10.1529/biophysj.106.096495

were purchased from Avanti Polar Lipids (Alabaster, AL). Cholesterol and *n*-octyl β-D-glucopyranoside were obtained from Sigma (St. Louis, MO). Cholesterol was recrytallized three times and stored under nitrogen at −20°C until needed. Tris-buffered saline (TBS) (10 mM Tris/100 mM NaCl, pH 7.2) and organic solvents were obtained from VWR (West Chester, PA). Dialysis cassettes (0.5–3 ml, Slide-A-Lyzer, 3500 MW cutoff) were purchased from Pierce (Rockford, IL). AFM cantilevers were purchased from Veeco (model MLCT-AUHW, part 00-103-0925; Woodbury, NY), and the largest V-shaped cantilever with a nominal spring constant (κ) 10 mN/m was used in all experiments (unless mentioned otherwise) after attachment of the glass microbead (~50 μm diameter, Polysciences, Warrington, WA). Where specified, in some cases the stiffer V-shaped cantilever (third from largest; $\kappa = 100$ mN/m) was used to accomplish higher compression forces. Purified water (18 MΩ-cm) was obtained from a NANOpure ultraviolet (UV) water purification system (Barnstead; Dubuque, IA).

Atomic force microscope

We used a custom-built AFM, in which the lateral and vertical scans are decoupled (35). In brief, the sample sits on an X-Y stage that can be adjusted relative to the cantilever mounted on a stacked piezo-electric transducer (Physik Instrumente L.P., Auburn, MA). The piezo-electric transducer provides the necessary vertical movement (from 0 to ~10 μm range) to approach and retract the cantilever from the stationary substrate (sample). Custom software was used to calibrate the cantilever tip based on thermal noise analysis (36), and to control the position of the piezo-electric transducer and timing during force scan measurements. A charge-coupled device camera was used to visualize the sample through a 20× objective positioned beneath the stage. For temperature experiments, a Peltier element was positioned underneath the sample chamber and a silicone-based heat sink compound was used to provide thermal coupling with the glass dish (sample). A temperature probe was positioned in direct contact with the sample and temperature stability was within 0.3°C.

AFM measurement of fusion force

During an AFM force scan measurement, the approach and retract traces correspond to the movement of the cantilever tip toward and away from the sample (substrate), respectively. As the cantilever is lowered and pressed against the substrate, the cantilever is subjected to forces that result in its bending (deflection). Deflection of the cantilever is monitored by the position of a pigtail laser beam focused on the coated back side of the cantilever tip and reflected onto a two-segment photodiode. Upward or downward cantilever deflections signify, respectively, repulsive or attractive interaction forces between the cantilever tip and the sample. The laser position change on the photodiode is calibrated based on the force causing the cantilever deflection. The interaction force between the cantilever and the sample is derived from the product of the spring constant (κ) of the cantilever, and the extent of its deflection. The resulting force scan represents the interaction force versus displacement of the piezo-electric transducer. Because fusion of the compressed bilayers occurs during the approach step, in this study, we focus on the approach trace and the fusion force is measured at the point where fusion is observed (Fig. 1).

Glass dish and cantilever preparation

Glass microbeads were epoxied to the tip of the silicone nitride cantilevers with the aid of a micromanipulator. Glass dishes and stainless steel utensils were boiled in distilled water containing ~10% RBS 35 detergent (Pierce) and ethanol, and rinsed extensively with distilled water. Cantilevers with attached microbeads were soaked in 1% *n*-octyl β-D-glucopyranoside, then in 100% ethanol followed by UV irradiation after extensive rinsing in nanopure water. Finally and immediately before use, cleaned cantilevers and glass dishes were further treated for 5 min in a nitrogen-plasma cleaner (Harrick Plasma; Ithaca, NY).

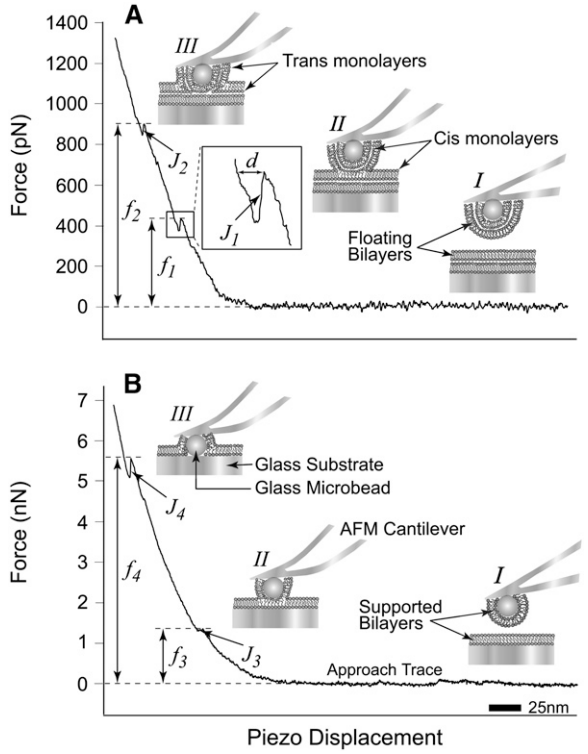

FIGURE 1 Illustrations (*I–III* (*A* and *B*); not to scale) and typical AFM force scans (force versus piezo-displacement) in the presence of floating (*A*) and supported (*B*) lipid bilayers showing the jumps ($J_{1\text{-}4}$) and the associated fusion forces ($f_{1\text{-}4}$). Force scans in panels *A* and *B* show that initially no interaction is taking place between the bilayers at long distances (*I*) and therefore the force is equal to zero. Upon further approach, the cantilever is bent as the bilayers start to press against one another and the force starts to increase. With the continued application of force, the bilayers are compressed together until fusion takes place (*II*) and a first jump (J_1 or J_3) is observed at ~450 pN (f_1) or ~1.4 nN (f_3), respectively. The jump is the result of the sudden movement of the cantilever tip toward the substrate as fusion of the floating bilayers (*A*) or supported bilayers (*B*) takes place (see illustrations). The piezo-electric transducer displacement (*d*, *inset*) during the jump is a measure of its distance and reflects the thickness of the fused bilayer. A transient reduction in force takes place as the cantilever tip relaxes during the jump, followed by an increase upon further bending with the continued application of compression, which eventually leads to the appearance of a second jump (J_2 or J_4) at ~900 pN (f_2) or ~5.5 nN (f_4), which is indicative of the fusion of the remaining floating bilayer (*A*) or supported (*B*), respectively (*III*).

Lipid vesicle reconstitution and floating bilayer formation

Lipid vesicles were prepared by the detergent depletion method with modifications (15,37,38). In brief, an appropriate amount of egg PC or DMPC solution was added to a cleaned round-bottom glass tube and the solvent was evaporated under a gentle stream of nitrogen and further treated under vacuum for at least 1 h. Dried lipids were hydrated in 0.5 ml 1% *n*-octyl β-D-glucopyranoside (55°C) by vortexing for a few minutes until the deposited lipid film was completely dissolved. Then 1.5 ml of TBS (55°C) was added while vortexing and further mixed for at least 2 min. The final

lipid concentrations of egg PC and DMPC vesicle suspensions were 1.25 and 1.5 mM, respectively. The vesicle suspension was then transferred into dialysis cassettes. Dialysis was done overnight in 3500 ml of TBS at 4°C for egg PC and at room temperature for DMPC. When cholesterol was included, appropriate amounts to yield the desired mol % were added to the egg PC solution in a round-bottom glass tube and mixed well before solvent evaporation. The dialyzed vesicle solution was collected and filtered, using a TBS-hydrated Acrodisc 25-mm syringe filter with 0.2 μm SUPOR membrane (PALL Life Sciences; Ann Arbor, MI), into a 3.5-ml VARI-CLEAN glass vial (Pierce). Vesicle suspensions were kept at 4°C and usually used within 5 days from preparation.

Floating bilayers were formed by vesicle adsorption and fusion onto hydrophilic glass surfaces (i.e., dish and microbead) (30,32). Vesicle solution (200 μl) was added to the preassembled AFM chamber. Adsorption was allowed to take place over the course of at least 1 h at room temperature. After the adsorption period, necessary temperature adjustments were made and the system was allowed to stabilize for another 10–15 min. Unless specified, force measurements were carried out in the presence of free vesicles in the chamber. During the entire course of the experiment, the constant presence of free vesicles was needed to sustain the floating bilayers.

RESULTS

AFM detection and identification of floating bilayers

Using AFM, we investigated interactions and measured forces required to induce fusion between floating bilayers. Floating lipid bilayers were formed on both, the glass substrate (dish) and the glass microbead attached to the AFM cantilever tip. In a typical AFM force scan measurement, the floating bilayers were brought into close apposition and compressed against one another during approach of the cantilever (microbead) toward the substrate (Fig. 1). When the applied force increased sufficiently to overcome a certain energy barrier, a jump (J_1) was observed in the approach trace. The jump is due to the sudden movement of the AFM tip toward the substrate as a result of the coalescence of material in the space between the microbead and the dish. For egg PC bilayers, the measured jump distance was 5.4 $\pm$ 0.2 nm, which is in the order of reported thickness values of a hydrated egg PC bilayer (8,39–41). Similarly, the jump (3.4 $\pm$ 0.2 nm) measured for DMPC bilayers was consistent with previously reported values of DMPC bilayer thickness (42–45). We and others interpret the jump as the result of fusion of the apposing floating bilayers into one floating bilayer (23). In this article, we will refer to this process as fusion. The newly formed floating bilayer consists of the distal (*trans*) monolayers of the fused bilayers (see illustration *II* in Fig. 1 *A*). The fusion force (f_1) is measured at the beginning of the jump. With further increase in applied force, a second jump (J_2) was observed at a higher force (f_2) suggesting the fusion of the remaining floating bilayer (Fig. 1 *A*). Although we use the term fusion to describe both events, they should not be confused as identical. During J_1, disruption of interactions among the hydrophobic tails (46–48) of phospholipid molecules within the floating bilayers is taking place, whereas, during J_2 interactions between polar headgroups in the apposing bilayers are disrupted.

To induce the fusion of the supported egg PC bilayers, higher compression forces were applied (Fig. 1 *B*). These experiments were conducted with stiffer AFM cantilevers to achieve higher compression forces. They were also carried out in the absence of free vesicles by washing excess nonadsorbed vesicles to ensure the presence of supported bilayers only. Force scans from these experiments revealed two jumps (J_3 and J_4), with similar jump distances to J_1 and J_2. These jumps occurred at much higher compression forces in the range of a few nanonewtons (f_3 and f_4), which is consistent with previously reported fusion forces for supported bilayers (8,44,45). It should be noted, however, that force scans from these experiments did not show the first two jumps (J_1 and J_2) associated with floating bilayers, which were removed by excessive washing of the sample chamber. Control experiments conducted without washing excess vesicles did occasionally show four consecutive jumps believed to be associated with both floating and supported bilayers. However, the majority of force scans from these experiments showed two jumps associated only with supported bilayers. A prerequisite for floating bilayers formation is the presence of supported bilayers; therefore, we believe that floating bilayers rarely existed between force scans in these control experiments. Taken together, these results suggest that the fusion forces f_1 and f_2 are associated with floating bilayers.

Because the focus of this study is on floating bilayers, we conducted all experiments using the softer AFM cantilevers, and only forces associated with the first jump (J_1) were reported. We typically collected ~3300 force scan measurements for each experiment (~300 scans per compression rate), and experiments were done in triplicates for each reported condition. Approximately 30% of force scans produced fusion events at low compression forces, which were randomly distributed throughout the experiments. These selected measurements were associated with interactions between two floating bilayers. The remaining 70% of scans lacking jump events at such lower compression forces are believed to have been acquired from either a single floating bilayer or supported bilayers only. Additional control experiments, where lipid bilayers were formed only on one of the substrates (dish or microbead) were performed. A single jump was observed in either case, indicating the presence of a single floating bilayer.

Dynamic force of bilayer fusion

To reveal the dynamic force spectrum of the fusion process between apposing floating bilayers, we carried out AFM force measurements at different compression rates. Compression rate is calculated by multiplying the cantilever spring constant (κ) by the scan velocity, and different compression rates were achieved by varying the scan velocity during approach of the AFM cantilever tip toward the substrate. A pronounced dependence of the fusion force on the compression rate was observed (Fig. 2). In general,

the forces ranged from ~100 to ~500 pN at compression rates from ~1000 to ~100,000 pN/s (Figs. 3 and 4). Our measurements revealed that the fusion force is proportional to the natural logarithm of the compression rate (i.e., plot f^* versus $\ln\{r_f\}$). As we will further elaborate below (see Discussion and Conclusions), this trend is consistent with a model where the energy barrier between the interacting bilayers decreases linearly with compression force. In this model, the activation energy barrier is characterized by two phenomenological parameters, k° and γ; k° and γ can be interpreted as the fusion rate of two contacting bilayers and the position of the transition state relative to an initial unfused state, respectively, in the absence of compression. Tables 1 and 2 list the k°- and γ-values derived from fitting this model to our AFM measurements. A similar phenomenological model was developed by Butt and Franz for the rupture of thin molecular films by AFM (49). The dynamic force spectra of the fusion process for both egg PC and DMPC bilayers (Figs. 3 and 4) revealed a single linear loading regime within compression rates accessible in our system. Based on our model, this is interpreted as evidence for the presence of a single energy barrier in the fusion of the lipid bilayers.

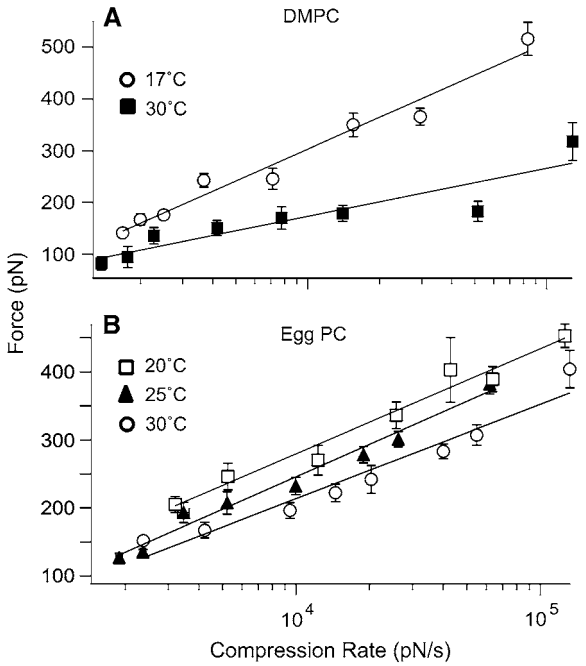

FIGURE 3 Force versus compression rate plots obtained in the presence of DMPC (*A*) or egg PC (*B*) floating bilayers at different temperatures. Solid lines are linear fits of the kinetic model. Error bars are the standard error of the mean.

Temperature effect on fusion of bilayers

Bilayer fluidity and phase transition are directly linked to temperature. We first tested the effect of temperature on the fusion force. Table 1 summarizes the results obtained from these experiments in terms of the fusion energy barrier parameters (k° and γ). In the presence of DMPC floating bilayers (melting temperature (*Tm*) of ~23°C), we carried out fusion force scan measurements above and below *Tm* at compression rates from ~1000 to ~100,000 pN/s. A significant change in the fusion force was observed between 17 and 30°C (Fig. 3 *A*). The dynamic force spectra revealed that the fusion energy barrier width (γ) increased by more than twofold (~0.6 Å) when the temperature was increased to 30°C. However, the height of the energy barrier (characterized by k°) was reduced by a negligible amount when DMPC bilayers were heated above *Tm* (Table 1). For egg PC floating bilayers, we carried out force scan measurements at 20, 25, and 30°C and the corresponding dynamic force spectra were revealed. We observed a moderate change in fusion force (Fig. 3 *B*). The barrier width (γ) remained nearly constant in the tested temperature range, whereas, the barrier height decreased by ~1.0 k_BT between 20 and 30°C (Table 1).

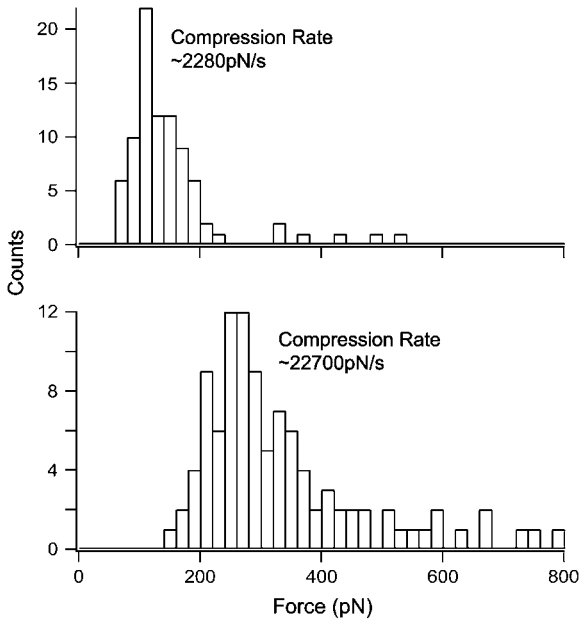

FIGURE 2 Representative force histograms of fusion forces for egg PC floating bilayers containing 10% cholesterol obtained at two different compression rates. The force increased with the compression rate.

Cholesterol effects on fusion force

Interactions between bilayers have been shown to vary widely with lipid composition (50–52). We investigated the effect of lipid composition on the fusion force in egg PC floating bilayers by adding cholesterol at 5–67% (mol). Force measurements were carried out at 24 ± 1°C. Fig. 4 shows the dynamic force spectra for fusion reactions between floating bilayers prepared with egg PC containing 0,

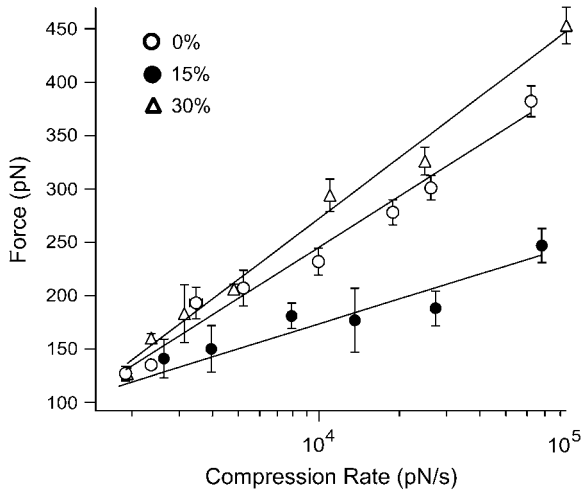

FIGURE 4 Force versus compression rate plots obtained in the presence of egg PC alone (0% chol) and egg PC floating bilayers containing 15% and 30% (mol) cholesterol. Solid lines are linear fits of the kinetic model. A downward shift in the dynamic force spectrum was observed in the presence of 15% cholesterol and fusion forces were reduced by ~50% at higher compression rates. Refer to supplemental Figs. S1 and S2 (Supplementary Material) for a comprehensive look at representative low, intermediate, and high cholesterol concentrations as compared to egg PC bilayers containing 0% cholesterol (supplemental Fig. S1). Error bars are mean ± SE.

15, and 30% cholesterol, respectively. For 30% cholesterol/egg PC bilayers, we did not observe a significant change in the dynamic force spectrum relative to egg PC-only (0% chol) bilayers. However, suppression in fusion force was observed at 15% cholesterol, especially, at the higher compression rates. Supplemental Fig. S1 (see Supplementary Material) shows a compilation of representative dynamic force spectra for the fusion reaction for low, intermediate, and high cholesterol-containing egg PC bilayers as compared to egg PC alone (0% chol) bilayers. Supplemental Fig. S2 (Supplementary Material) shows additional force versus compression rate plots derived at 10, 25, 40, and 67% cholesterol. Results from all experiments conducted with different cholesterol concentrations are summarized in Table 2, where derived fusion energy barrier parameters ($k°$ and γ) are presented.

DISCUSSION AND CONCLUSIONS

Our work focused on floating lipid bilayers, which have been suggested to be more comparable to biological membranes

TABLE 1 Fusion energy barrier parameters for floating bilayers derived at different temperatures

	Egg PC			DMPC	
°C	20	25	30	17	30
γ (Å)	0.60	0.61	0.69	0.45	1.04
$k°$ (s^{-1})	2.32	4.06	4.79	3.70	3.36

$k°$ characterizes the height of the potential and γ describes its width.

TABLE 2 Fusion energy barrier parameters for egg PC floating bilayers containing different mol % cholesterol

% Chol	5	10	15	20	25	30	40	67
γ (Å)	0.58	0.53	1.21	1.04	0.77	0.50	0.32	0.37
$k°$ (s^{-1})	2.59	2.38	1.73	2.03	2.24	4.47	2.47	3.13

than supported bilayers (27,28). We report here on the development and characterization of a lipid bilayer system, aimed at investigating the fusion of floating bilayers. Force measurements of interactions between apposing bilayers and fusion events were generated using the AFM. This system provided the sensitivity to detect transitions on the nanoscale and measure forces required to induce fusion between supported and floating lipid bilayers. Bilayer formation on the AFM tip was accomplished by attaching glass microbeads to the cantilever tips. Lipid vesicles readily adsorb and fuse to hydrophilic surfaces to form bilayers (15,38,41,53–56). However, for lipid vesicles to adsorb, the adsorption energy must be higher than the bending energy of the bilayer (57). The minimal curvature radius of a bilayer was calculated to be between 32 and 100 nm based on adsorption energies of 2×10^{-4} and 0.2×10^{-4} J/m^2, respectively (23). The beads we used had an average diameter of ~50 μm. The hydrophilic nature of our substrates was confirmed by the presence of electrostatic repulsion when performing scans in pure water between glass dishes and glass microbeads attached to the cantilever tips (data not shown). It has been suggested that pursuant to adsorption, lipid vesicles collapse and the stacked sides of the collapsed vesicles form double bilayers (a floating bilayer on top of a supported one). The top floating bilayer eventually slides along the bottom bilayer and expands it laterally forming a larger single supported bilayer (6,58). In our system, however, this lateral movement may be impeded by the presence of neighboring vesicles undergoing the same process, which causes the top layers to remain in place due to space constraints and results in floating bilayers. The constant supply of free vesicles helps sustain the floating bilayers on both the microbead and dish.

We showed that apposing floating bilayers were present in ~30% of the force scans, and we only reported fusion forces associated with floating bilayers. We speculate that the remaining 70% of force scans lacking jump events were carried out on supported bilayers (with or without a single floating bilayer) or on bare glass surfaces. However, we do not think the latter is likely due to the random distribution of fusion events for floating bilayers, which indicates that supported bilayers were present for floating bilayers to have existed. Moreover, compression forces applied during force measurements were not sufficient to induce fusion of supported bilayers, let alone removing them from the substrates. On the other hand, as previously reported (51,59,60), we express no concerns with bilayer aging since the jump distance remained consistent for the duration of each experiment (data not shown).

In this study, the dynamic force spectra for fusion of floating bilayers at different lipid compositions and temperatures were revealed by carrying out fusion force measurements over a range of compression rates. A clear dependence of the fusion force on the compression rate was observed. The force ranged from ~100 to ~500 pN for compression rates between ~1000 and ~100,000 pN/s. These forces are in the range of previously reported fusion force values measured in floating bilayers by AFM (28). We assume that the fusion process follows a linear activation potential and a single loading regime was identified in DMPC and egg PC bilayers in all tested conditions. This suggests that the kinetics of fusion of floating bilayers is governed by one main energy barrier under these conditions. The observed increase in fusion force with the log of the compression rate is consistent with a linear intersurface potential leading up to the fusion event. In this model, we assume that the kinetics of the fusion process is given by

$$k = C\exp\left\{\frac{-\Delta G^{*}}{k_{\mathrm{B}}T}\right\}, \quad (1)$$

where ΔG^{*} is the activation energy, T is the absolute temperature, k_{B} is Boltzmann's constant, and C is a phenomenological constant that depends on the experimental system. When the membranes are subjected to a compression force f, the force will add a term to the thermopotential of the system. If the potential barrier is steep, the addition of this term to the free energy will reduce the barrier by an amount of $f\gamma$, where γ is the distance between the unfused bilayers and the transition state positions along the reaction coordinate. Thus, the fusion rate under compression is

$$k(f) = C\exp\left\{\frac{-(\Delta G^{*} - f\gamma)}{k_{\mathrm{B}}T}\right\} = k^{\circ}\exp\left\{\frac{f\gamma}{k_{\mathrm{B}}T}\right\}, \quad (2)$$

where k° is the fusion rate constant in the absence of compression.

Equation 2 describes how the fusion rate is changed by constant compression forces. However, a constant compression force is difficult to maintain in an AFM experiment. Instead, a dynamic force approach was used to characterize the forces leading to fusion of the compressed bilayers. Under conditions of constant compression rate r_{f} ($r_{\mathrm{f}} = df/dt$), the probability density function for forced fusion is given by

$$P(f) = k^{\circ}\exp\left\{\frac{\gamma f}{k_{\mathrm{B}}T}\right\}\exp\left\{\frac{k^{\circ}k_{\mathrm{B}}T}{\gamma r_{\mathrm{f}}}\left[1 - \exp\left(\frac{\gamma f}{k_{\mathrm{B}}T}\right)\right]\right\}, \quad (3)$$

and the most probable force f^{*} (i.e., the maximum of the distribution $\partial P(f)/\partial f = 0$) can be expressed as

$$f^{*} = \frac{k_{\mathrm{B}}T}{\gamma}\ln\left\{\frac{\gamma}{k^{\circ}k_{\mathrm{B}}T}\right\} + \frac{k_{\mathrm{B}}T}{\gamma}\ln\{r_{\mathrm{f}}\}. \quad (4)$$

Equation 4 shows that the most probable fusion force f^{*} is a linear function of the natural logarithm of the compression rate $\ln\{r_{\mathrm{f}}\}$. The fusion parameters k° and γ were derived from fitting Eq. 4 to the acquired plots of f^{*} versus $\ln\{r_{\mathrm{f}}\}$, which we refer to as the ''dynamic force spectrum''. Tables 1 and 2 list the k° and γ values for fusion reactions of floating lipid bilayers under the specified conditions.

Our study revealed that interactions between floating bilayers are strongly dependent on temperature and lipid composition (50,61). Both parameters directly influence the fluidity and phase transition of bilayers. Fig. 5 illustrates our

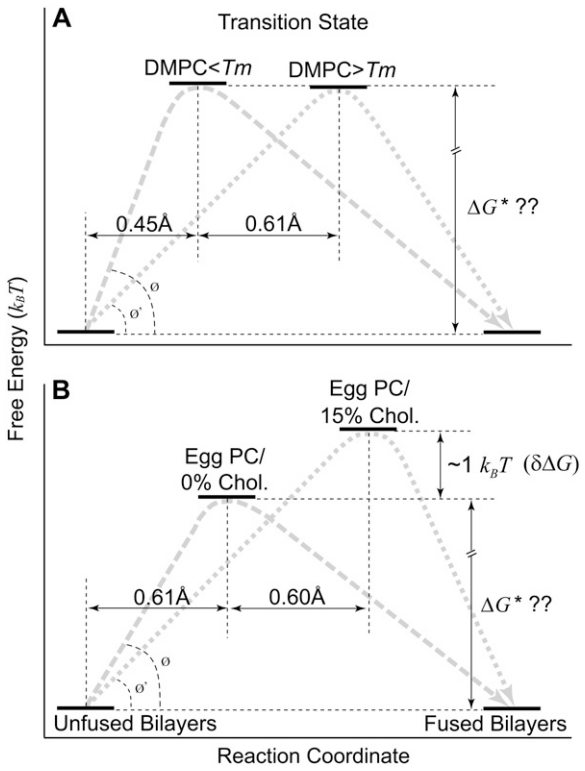

FIGURE 5 Schematic depiction (not to scale) of the energy landscape of the fusion process in DMPC (*A*) and egg PC (*B*) floating bilayers and its change with temperature and lipid composition as interpreted based on the kinetic model (see Discussion and Conclusions). During compression of apposing individual floating bilayers, they have to pass (along *gray dashed* and *dotted lines*) through a transition state that is at the peak of an energy barrier ΔG^{*} (Eq. 2). Arbitrary positions along the free energy axis were chosen for the unfused or fused bilayers since it is unknown which one has the lower free energy minimum. As a reference point along the reaction coordinate, we use the initial state (unfused) where compressed individual floating bilayers still exist. An arbitrary position assigned to the transition state in the presence of egg PC bilayers (0% chol at 25°C) was used as a reference point along the y axis. We use Eq. 5 to determine the relative difference $\delta\Delta G$ between two conditions of the same lipids. (*A*) No significant change in the barrier height was observed with temperature for DMPC floating bilayers (see Table 2). On the other hand, a pronounced widening (~0.61 Å) in the barrier was observed when DMPC bilayers were heated above *Tm* to 30°C. (*B*) Similarly, when 15% cholesterol was introduced to egg PC bilayers, a twofold increase in the energy barrier width was observed. Moreover, we calculated a ~1.0 $k_{\mathrm{B}}T$ increase in the activation energy for 15% cholesterol/egg PC bilayers compared to that for bilayers prepared with egg PC alone or egg PC/cholesterol at low and high concentrations. In both panels *A* and *B*, notice the overall decrease in the slope of the energy barrier, as represented by the angle change between Ø and Ø′.

interpretation of the results and helps put the derived energy barrier parameters (k° and γ) in perspective. In general, for apposing bilayers to fuse, an energy barrier must be overcome before intimate contact can be established and fusion can occur. However, fusion of the interacting bilayers can be accelerated in the presence of applied compression. As the interacting bilayers move toward the fused state, they pass through a transition state at the peak of the energy barrier. Using this model, the derived barrier parameters allowed us to estimate the position of the transition state where relative differences in the height and width of the energy barrier between lipid systems under different conditions can be compared. The relative difference in the energy barrier height $\delta\Delta G$ between two similar systems is given by

$$\delta\Delta G = -k_B T \ln\left(\frac{k^\circ_1}{k^\circ_2}\right), \quad (5)$$

where k°_1 and k°_2 are the fusion rate constants of the compared systems 1 and 2, respectively.

Fig. 5 *A* compares the interaction energetics of DMPC floating bilayers in both the gel (17°C) and fluid (30°C) phase, in the absence of applied compression. The most striking difference between the potentials is a shift in the position, along the reaction coordinate, of the transition state to a much higher value at the higher temperature, where DMPC bilayers are in the fluid state. Surprisingly, the heights of the barriers were not significantly affected (Table 1). This indicates that phase transition from gel to liquid phase affected the energy barrier by making it wider and consequently less steep, which yielded lower fusion forces under compression. A steeper energy barrier is mechanically more difficult to overcome; hence, the higher fusion forces below *Tm* (Fig. 3 *A*). On the other hand, for egg PC bilayers, the fusion energy barrier width remained nearly constant, whereas, its height was reduced by $\sim$1.0 k_BT between 20 and 30°C (Table 1). The melting temperature for egg PC is ~-15°C (43,59,62). Therefore, no phase transition is expected in the tested temperature range. However, an increase in the thermal fluctuation of the bilayers is likely with a temperature increase from 20 to 30°C (43), and hence a moderate increase in bilayer fluidity. This indicates that in the absence of applied compression, modest increases in fluidity of egg PC bilayers within the same physical state (i.e., fluid) due to increased thermal fluctuation, yielded lower fusion activation energy by reducing the height of the energy barrier, whereas, temperature changes across the phase transition resulted in lower fusion forces for DMPC bilayers by widening the energy barrier (Table 1). It is not clear why there was a differential effect on the barrier width across the phase transition temperature for DMPC bilayers. Similarly, anomalous transition behaviors of 1,2-dipalmitoyl-*sn*-glycero-3-phosphotidylcholine bilayers have been reported around *Tm* (29). One possibility for not seeing widening of the energy barrier for egg PC bilayers is the big difference between *Tm* and the tested temperatures, where a change of 10° had a modest effect on fluidity compared to that of cholesterol. Nevertheless, the overall trend of temperature effect is a reduction in the slope of the energy barrier, which consequently facilitated the fusion process in the absence and presence of applied compression.

Cholesterol affects packing of phospholipid molecules in bilayers, which, in turn, affects their fluidity (52,63–67). Fig. 5 *B* compares the interaction energetics of egg PC floating bilayers with and without cholesterol. Our results showed that intermediate cholesterol concentrations resulted in widening of the energy barrier (1.21, 1.04, and 0.77 Å at 15, 20, and 25%, respectively; Table 2). The observed widening in the energy barrier can be attributed to the effect of cholesterol on the transition temperature. Transition temperature of lipid bilayers in the fluid state has been shown to decrease with increasing cholesterol content (68). On the other hand, our data showed that 15, 20, and 25% cholesterol increased the height of the energy barrier by $\sim$1.0 k_BT compared to that of floating bilayers of egg PC alone or egg PC bilayers containing other cholesterol concentrations. Although, both the barrier height and width were increased at intermediate cholesterol concentrations, the fusion force was decreased. This suggests that, despite the fact that both parameters (i.e., height and width) do affect the slope of the fusion energy barrier, the barrier width seems to have a more prevalent effect on the fusion process and its impact becomes more pronounced during accelerated fusion under applied compression. It is noted that our intermediate cholesterol concentrations, which changed the fusion energy barrier parameters, are in agreement with previously reported values in fluid lipid membranes, where different dynamic properties of the membrane were reported for additions of $\sim$30 mol % cholesterol (68,69).

We measured an average jump distance of 4.2 $\pm$ 0.5 nm for egg PC bilayers containing cholesterol. We speculate that the smaller jump distance is due to further proximity between apposing bilayers during compression perhaps through interpenetration of the less-packed headgroups in the opposite floating bilayers as a result of reduced steric pressures (70). Another possibility may lie in the hydration level of the bilayers. As much as a 15-Å change in thickness of the separating water layers between bilayers of egg PC or DMPC has been measured under various osmotic pressures (43). It has also been reported that the thickness of water layers between fluid bilayers and bilayer/substrate changes ($\sim$5 Å) with different cholesterol contents (71). Our data show a difference of $\sim$12 Å in jump distance for egg PC bilayers with and without cholesterol, which is in agreement with previously reported values. With the assumption that the bilayer hydrocarbon thickness is constant and that the jump is the actual displacement of the AFM cantilever tip toward the substrate, the jump distance in presence of cholesterol would have been reduced by either, the amount of interpenetration or the reduced water layers thickness between interacting bilayers, or both simultaneously.

Despite the reduction in the fusion force at intermediate cholesterol concentrations, we attribute the increase in the activation energy to a change in the interaction forces that contribute to the energy barrier. Major contributors to the fusion energy barrier are thought to be the steric, hydration, and double layer repulsions that exist between polar headgroups of phospholipid molecules in the opposite bilayers (45,50,51). First, when the separating water layer thickness between apposing bilayers is decreased, the work of dehydration associated with the removal of water molecules from the interface would be expected to decrease, which may lead to lower activation energy. Second, in addition to its effects on steric hindrance, cholesterol has been shown to organize water layers surrounding headgroups of phospholipid molecules (70). Although reducing steric repulsion helps lower fusion energy requirements, increased organization of water molecules increases hydration repulsion, which tends to increase the activation energy. This is consistent with our data where the barrier height generally increased in the presence of cholesterol compared to egg PC alone at 25°C. However, such an effect appeared to be more pronounced at intermediate cholesterol concentrations for reasons we currently do not understand. Moreover, although the jump distance was reduced to a similar extent in all tested cholesterol concentrations, only intermediate values resulted in lower fusion force under applied compression to the bilayers. As suggested above, this is due to the reduced slope of the energy barrier as a result of the increase in its width. Taken together, this suggests that cholesterol at intermediate concentrations, has added effects on the energy barrier between apposing bilayers yielding a higher but less-steep fusion energy barrier (Fig. 5 *B*). In the absence of applied compression, such a higher barrier would be more difficult to overcome; hence the slower fusion rate (Table 2). However, given the lower slope, fusion forces would be lower during accelerated fusion under applied compression. Similar cholesterol concentrations have been reported to have pronounced effects on lateral diffusion and transition temperature in bilayers (66,72,73).

Our AFM lipid bilayer system allowed the detection of nanoscale jump distances and the measurement of fusion forces in supported and floating bilayers. In addition, it provided the ability to detect and quantify changes in the fusion energy landscape associated with bilayer fluidity and overall changes in the forces dominating the fusion energy barrier. The applied compression mimics forces contributed by specialized fusion proteins in vivo. Fusion proteins such as soluble *N*-ethylmalimide-sensitive factor attachment protein receptor (SNAREs) bring vesicles into close contact with the plasma membrane of neuronal cells where fusion and neurotransmitter release take place after certain stimuli (i.e., increased cytosolic Ca^{2+}). SNAREs are thought to be the in vivo minimal fusion machinery (37) contributing the necessary mechanical work to bring interacting membranes over the energy barrier, where lipid mixing and rearrangement (i.e., fusion) may take place (74). The dynamic force spectra for bilayer fusion reactions can be obtained in the presence of different fusogens (e.g., SNAREs) and differences in energy requirements to induce fusion can determine their relative contributions into the total energy of the process. Recently, cholesterol was proposed to be a critical component of the minimal fusion machinery due to its positive roles in membrane fusion (75). Using our system, we were able to reveal the promoting effect of intermediate concentrations of cholesterol on the fusion process. Even though our results showed a reduced fusion rate in the absence of compression, membrane fusion is, nevertheless, an active process and spontaneous fusion events are very rare (74). Docked synaptic vesicles remain poised next to the presynaptic membrane until a stimulus is received (50). Although spontaneous asynchronous release does occur physiologically, it remains an active process driven by fusion proteins triggered by localized increases in free Ca^{2+} at the fusion sites. Consistent with the proposition of the crucial role of cholesterol in membrane fusion, and the notion that SNAREs contribute the required mechanical energy necessary for fusion in vivo, we showed that the overall effect of intermediate cholesterol concentrations facilitated fusion under compression in our system. With further development, this system may indeed prove instrumental in the investigation and establishment of mechanisms of membrane fusion.

SUPPLEMENTARY MATERIAL

An online supplement to this article can be found by visiting BJ Online at http://www.biophysj.org.

We thank C. Freites for custom fabrications and B. Yuan and M. Hôefling for help with software development. We also thank Drs. F. Rico and E. P. Wojcikiewicz for insightful feedback.

This work was supported by a grant from National Institutes of Health (GM55611).

REFERENCES

1. Blumenthal, R., M. J. Clague, S. R. Durell, and R. M. Epand. 2003. Membrane fusion. *Chem. Rev.* 103:53–69.
2. Chernomordik, L. V., and M. M. Kozlov. 2003. Protein-lipid interplay in fusion and fission of biological membranes. *Annu. Rev. Biochem.* 72:175–207.
3. Fardon, N. J., R. Wilkinson, and T. H. Thomas. 2001. Rapid fusion of granules with neutrophil cell membranes in hypertensive patients may increase vascular damage. *Am. J. Hypertens.* 14:927–933.
4. Lentsch, A. B., and P. A. Ward. 2000. Regulation of inflammatory vascular damage. *J. Pathol.* 190:343–348.
5. Rand, R. P., and V. A. Parsegian. 1986. Mimicry and mechanism in phospholipid models of membrane fusion. *Annu. Rev. Physiol.* 48: 201–212.
6. Kalb, E., S. Frey, and L. K. Tamm. 1992. Formation of supported planar bilayers by fusion of vesicles to supported phospholipid monolayers. *Biochim. Biophys. Acta.* 1103:307–316.
7. Heyse, S., H. Vogel, M. Sanger, and H. Sigrist. 1995. Covalent attachment of functionalized lipid bilayers to planar waveguides for

measuring protein binding to biomimetic membranes. *Protein Sci.* 4: 2532–2544.

8. Mueller, H., H. J. Butt, and E. Bamberg. 1999. Force measurements on myelin basic protein adsorbed to mica and lipid bilayer surfaces done with the atomic force microscope. *Biophys. J.* 76:1072–1079.
9. Subczynski, W. K., and A. Wisniewska. 2000. Physical properties of lipid bilayer membranes: relevance to membrane biological functions. *Acta Biochim. Pol.* 47:613–625.
10. Tokumasu, F., A. J. Jin, G. W. Feigenson, and J. A. Dvorak. 2003. Nanoscopic lipid domain dynamics revealed by atomic force microscopy. *Biophys. J.* 84:2609–2618.
11. Dufrene, Y. F., and G. U. Lee. 2000. Advances in the characterization of supported lipid films with the atomic force microscope. *Biochim. Biophys. Acta.* 1509:14–41.
12. Jass, J., T. Tjarnhage, and G. Puu. 2003. Atomic force microscopy imaging of liposomes. *Methods Enzymol.* 367:199–213.
13. Richter, R. P., and A. R. Brisson. 2005. Following the formation of supported lipid bilayers on mica: a study combining AFM, QCM-D, and ellipsometry. *Biophys. J.* 88:3422–3433.
14. Binnig, G., C. F. Quate, and C. Gerber. 1986. Atomic force microscope. *Phys. Rev. Lett.* 56:930–933.
15. Jass, J., T. Tjarnhage, and G. Puu. 2000. From liposomes to supported, planar bilayer structures on hydrophilic and hydrophobic surfaces: an atomic force microscopy study. *Biophys. J.* 79:3153–3163.
16. Jena, B. P. 2003. Fusion pore or porosome: structure and dynamics. *J. Endocrinol.* 176:169–174.
17. Schneider, J., Y. F. Dufrene, W. R. Barger Jr., and G. U. Lee. 2000. Atomic force microscope image contrast mechanisms on supported lipid bilayers. *Biophys. J.* 79:1107–1118.
18. Hui, S. W., R. Viswanathan, J. A. Zasadzinski, and J. N. Israelachvili. 1995. The structure and stability of phospholipid bilayers by atomic force microscopy. *Biophys. J.* 68:171–178.
19. Kumar, S., and J. H. Hoh. 2001. Probing the machinery of intracellular trafficking with the atomic force microscope. *Traffic.* 2:746–756.
20. Manne, S., and H. E. Gaub. 1995. Molecular-organization of surfactants at solid-liquid interfaces. *Science.* 270:1480–1482.
21. Zhang, X., S. E. Craig, H. Kirby, M. J. Humphries, and V. T. Moy. 2004. Molecular basis for the dynamic strength of the integrin alpha4beta1/VCAM-1 interaction. *Biophys. J.* 87:3470–3478.
22. Wojcikiewicz, E. P., X. Zhang, and V. T. Moy. 2004. Force and compliance measurements on living cells using atomic force microscopy (AFM). *Biol. Proced. Online.* 6:1–9.
23. Pera, I., R. Stark, M. Kappl, H. J. Butt, and F. Benfenati. 2004. Using the atomic force microscope to study the interaction between two solid supported lipid bilayers and the influence of synapsin I. *Biophys. J.* 87: 2446–2455.
24. Worsfold, O., N. H. Voelcker, and T. Nishiya. 2006. Biosensing using lipid bilayers suspended on porous silicon. *Langmuir.* 22:7078–7083.
25. Daillant, J., E. Bellet-Amalric, A. Braslau, T. Charitat, G. Fragneto, F. Graner, S. Mora, F. Rieutord, and B. Stidder. 2005. Structure and fluctuations of a single floating lipid bilayer. *Proc. Natl. Acad. Sci. USA.* 102:11639–11644.
26. Kaizuka, Y., and J. T. Groves. 2004. Structure and dynamics of supported intermembrane junctions. *Biophys. J.* 86:905–912.
27. Fragneto, G., T. Charitat, F. Graner, K. Mecke, L. Perino-Gallice, and E. Bellet-Amalric. 2001. A fluid floating bilayer. *Europhys. Lett.* 53:100–106.
28. Maeda, N., T. J. Senden, and J. M. di Meglio. 2002. Micromanipulation of phospholipid bilayers by atomic force microscopy. *Biochim. Biophys. Acta.* 1564:165–172.
29. Stidder, B., G. Fragneto, and S. J. Roser. 2005. Effect of low amounts of cholesterol on the swelling behavior of floating bilayers. *Langmuir.* 21:9187–9193.
30. Giocondi, M. C., and C. Le Grimellec. 2004. Temperature dependence of the surface topography in dimyristoylphosphatidylcholine/distearoylphosphatidylcholine multibilayers. *Biophys. J.* 86:2218–2230.
31. Kaasgaard, T., C. Leidy, J. H. Crowe, O. G. Mouritsen, and K. Jorgensen. 2003. Temperature-controlled structure and kinetics of ripple phases in one- and two-component supported lipid bilayers. *Biophys. J.* 85:350–360.
32. Leidy, C., T. Kaasgaard, J. H. Crowe, O. G. Mouritsen, and K. Jorgensen. 2002. Ripples and the formation of anisotropic lipid domains: imaging two-component supported double bilayers by atomic force microscopy. *Biophys. J.* 83:2625–2633.
33. Wong, A. P., and J. T. Groves. 2002. Molecular topography imaging by intermembrane fluorescence resonance energy transfer. *Proc. Natl. Acad. Sci. USA.* 99:14147–14152.
34. Loi, S., G. Sun, V. Franz, and H. J. Butt. 2002. Rupture of molecular thin films observed in atomic force microscopy. II. Experiment. *Phys. Rev. E.* 66:031602.
35. Chen, A., and V. T. Moy. 2002. Single-molecule force measurements. *Methods Cell Biol.* 68:301–309.
36. Hutter, J. L., and J. Bechhoefer. 1993. Calibration of atomic-force microscope tips. *Rev. Sci. Instrum.* 64:1868–1873.
37. Weber, T., B. V. Zemelman, J. A. McNew, B. Westermann, M. Gmachl, F. Parlati, T. H. Sollner, and J. E. Rothman. 1998. SNAREpins: minimal machinery for membrane fusion. *Cell.* 92:759–772.
38. Tokumasu, F., A. J. Jin, G. W. Feigenson, and J. A. Dvorak. 2003. Atomic force microscopy of nanometric liposome adsorption and nanoscopic membrane domain formation. *Ultramicroscopy.* 97:217–227.
39. Liang, X., G. Mao, and K. Y. Simon Ng. 2004. Probing small unilamellar EggPC vesicles on mica surface by atomic force microscopy. *Colloids Surf. B Biointerfaces.* 34:41–51.
40. McIntosh, T. J., A. D. Magid, and S. A. Simon. 1987. Steric repulsion between phosphatidylcholine bilayers. *Biochemistry.* 26:7325–7332.
41. Horn, R. G. 1984. Direct measurement of the force between two lipid bilayers and observation of their fusion. *Biochim. Biophys. Acta.* 778:224–228.
42. Gordeliy, V. I., V. Cherezov, and J. Teixeira. 2005. Strength of thermal undulations of phospholipid membranes. *Phys. Rev. E.* 72:061913.
43. Petrache, H. I., S. Tristram-Nagle, and J. F. Nagle. 1998. Fluid phase structure of EPC and DMPC bilayers. *Chem. Phys. Lipids.* 95:83–94.
44. Helm, C. A., J. N. Israelachvili, and P. M. McGuiggan. 1992. Role of hydrophobic forces in bilayer adhesion and fusion. *Biochemistry.* 31: 1794–1805.
45. Marra, J., and J. Israelachvili. 1985. Direct measurements of forces between phosphatidylcholine and phosphatidylethanolamine bilayers in aqueous electrolyte solutions. *Biochemistry.* 24:4608–4618.
46. Helm, C. A., and J. N. Israelachvili. 1993. Forces between phospholipid bilayers and relationship to membrane fusion. *Methods Enzymol.* 220:130–143.
47. Haque, M. E., and B. R. Lentz. 2004. Roles of curvature and hydrophobic interstice energy in fusion: studies of lipid perturbant effects. *Biochemistry.* 43:3507–3517.
48. Leikin, S. L., M. M. Kozlov, L. V. Chernomordik, V. S. Markin, and Y. A. Chizmadzhev. 1987. Membrane fusion: overcoming of the hydration barrier and local restructuring. *J. Theor. Biol.* 129:411–425.
49. Butt, H. J., and V. Franz. 2002. Rupture of molecular thin films observed in atomic force microscopy. I. Theory. *Phys. Rev. E.* 66:031601.
50. Lis, L. J., M. McAlister, N. Fuller, R. P. Rand, and V. A. Parsegian. 1982. Interactions between neutral phospholipid bilayer membranes. *Biophys. J.* 37:657–665.
51. Wolfe, J., E. Perez, M. Bonanno, and J. P. Chapel. 1991. The interaction and fusion of bilayers formed from unsaturated lipids. *Eur. Biophys. J.* 19:275–281.
52. Li, X. M., M. M. Momsen, H. L. Brockman, and R. E. Brown. 2003. Sterol structure and sphingomyelin acyl chain length modulate lateral packing elasticity and detergent solubility in model membranes. *Biophys. J.* 85:3788–3801.
53. Schonherr, H., J. M. Johnson, P. Lenz, C. W. Frank, and S. G. Boxer. 2004. Vesicle adsorption and lipid bilayer formation on glass studied by atomic force microscopy. *Langmuir.* 20:11600–11606.

54. Wang, L., Y. Song, X. Han, B. Zhang, and E. Wang. 2003. Growth of cationic lipid toward bilayer lipid membrane by solution spreading: scanning probe microscopy study. *Chem. Phys. Lipids.* 123:177–185.

55. Johnson, J. M., T. Ha, S. Chu, and S. G. Boxer. 2002. Early steps of supported bilayer formation probed by single vesicle fluorescence assays. *Biophys. J.* 83:3371–3379.

56. Steinem, C., A. Janshoff, W. P. Ulrich, M. Sieber, and H. J. Galla. 1996. Impedance analysis of supported lipid bilayer membranes: a scrutiny of different preparation techniques. *Biochim. Biophys. Acta.* 1279:169–180.

57. Seifert, U., and R. Lipowsky. 1990. Adhesion of vesicles. *Phys. Rev. A.* 42:4768–4771.

58. Keller, C. A., and B. Kasemo. 1998. Surface specific kinetics of lipid vesicle adsorption measured with a quartz crystal microbalance. *Biophys. J.* 75:1397–1402.

59. Zhang, J. A., and J. Pawelchak. 2000. Effect of pH, ionic strength and oxygen burden on the chemical stability of EPC/cholesterol liposomes under accelerated conditions. Part 1: Lipid hydrolysis. *Eur. J. Pharm. Biopharm.* 50:357–364.

60. Parasassi, T., A. M. Giusti, M. Raimondi, G. Ravagnan, O. Sapora, and E. Gratton. 1995. Cholesterol protects the phospholipid bilayer from oxidative damage. *Free Radic. Biol. Med.* 19:511–516.

61. Simon, S. A., S. Advani, and T. J. McIntosh. 1995. Temperature dependence of the repulsive pressure between phosphatidylcholine bilayers. *Biophys. J.* 69:1473–1483.

62. Liang, X., G. Mao, and K. Y. Ng. 2004. Mechanical properties and stability measurement of cholesterol-containing liposome on mica by atomic force microscopy. *J. Colloid Interface Sci.* 278:53–62.

63. Karmakar, S., and V. A. Raghunathan. 2005. Structure of phospholipid-cholesterol membranes: An x-ray diffraction study. *Phys. Rev. E.* 71: 061924.

64. Radhakrishnan, A., and H. McConnell. 2005. Condensed complexes in vesicles containing cholesterol and phospholipids. *Proc. Natl. Acad. Sci. USA.* 102:12662–12666.

65. Terova, B., G. Petersen, H. S. Hansen, and J. P. Slotte. 2005. N-acyl phosphatidylethanolamines affect the lateral distribution of cholesterol in membranes. *Biochim. Biophys. Acta.* 1715:49–56.

66. Wu, E. S., and C. S. Yang. 1984. Lateral diffusion of cytochrome P-450 in phospholipid bilayers. *Biochemistry.* 23:28–33.

67. Tank, D. W., E. S. Wu, P. R. Meers, and W. W. Webb. 1982. Lateral diffusion of gramicidin C in phospholipid multibilayers. Effects of cholesterol and high gramicidin concentration. *Biophys. J.* 40:129–135.

68. Parasassi, T., A. M. Giusti, M. Raimondi, and E. Gratton. 1995. Abrupt modifications of phospholipid bilayer properties at critical cholesterol concentrations. *Biophys. J.* 68:1895–1902.

69. Hinz, H. J., and J. M. Sturtevant. 1972. Calorimetric investigation of the influence of cholesterol on the transition properties of bilayers formed from synthetic L- -lecithins in aqueous suspension. *J. Biol. Chem.* 247:3697–3700.

70. McIntosh, T. J., A. D. Magid, and S. A. Simon. 1989. Cholesterol modifies the short-range repulsive interactions between phosphatidylcholine membranes. *Biochemistry.* 28:17–25.

71. Stidder, B., G. Fragneto, R. Cubitt, A. V. Hughes, and S. J. Roser. 2005. Cholesterol induced suppression of large swelling of water layer in phosphocholine floating bilayers. *Langmuir.* 21:8703–8710.

72. Larsson, M., K. Larsson, T. Nylander, and P. Wollmer. 2003. The bilayer melting transition in lung surfactant bilayers: the role of cholesterol. *Eur. Biophys. J.* 31:633–636.

73. Filippov, A., G. Oradd, and G. Lindblom. 2003. The effect of cholesterol on the lateral diffusion of phospholipids in oriented bilayers. *Biophys. J.* 84:3079–3086.

74. McNew, J. A., T. Weber, F. Parlati, R. J. Johnston, T. J. Melia, T. H. Sollner, and J. E. Rothman. 2000. Close is not enough: SNARE-dependent membrane fusion requires an active mechanism that transduces force to membrane anchors. *J. Cell Biol.* 150:105–117.

75. Churchward, M. A., T. Rogasevskaia, J. Hofgen, J. Bau, and J. R. Coorssen. 2005. Cholesterol facilitates the native mechanism of Ca2+-triggered membrane fusion. *J. Cell Sci.* 118:4833–4848.